PROCEEDINGS OF SCIENCE

Diffuse neutral hydrogen in the Local Universe

Attila Popping
Laboratoire d'Astrophysique de Marseille
E-mail: attila.popping@oamp.fr

Numerical simulations predict that galaxies and clusters in the Local Volume are connected by extended diffuse filaments of gas. Although most of this gas is ionised, the peaks of this Cosmic Web should be detectable in H I 21-cm emission at very low column densities. Exploring the circum- and inter galactic medium is very important to understand accretion and feedback processes, which determine the evolution of galaxies. We have used a hydrodynamic simulation from which the neutral component is extracted and compared with observations. In a search for low surface brightness H I, three independent H I surveys have been conducted, using the WSRT both in total-power and cross-correlation mode and using re-processed HIPASS data. All three surveys have a very good brightness sensitivity at a different spatial resolution, which allows to distinguish very diffuse sources. We find a number of new H I detections without an obvious optical counterpart. These detections appear very diffuse and extended and are potentially traces of the Cosmic Web. Detecting diffuse neutral hydrogen with existing facilities is very hard and time consuming and the limits of current telescopes are being explored. The next generation of radio telescopes will be able to observe features as presented here more frequently and with more detail.

ISKAF2010 Science Meeting
June 10 -14 2010
Assen, the Netherlands

PoS(ISKAF2010)077

1. Introduction

Extragalactic astronomy has traditionally focused on the regions of extreme cosmic overdensity that we know as galaxies. In recent years the realization has emerged that galaxies do not dominate the universal baryon budget but are merely the brightest pearls of an underlying Cosmic Web. Simulations predict that baryons are equally distributed between galaxies, the Ly-α forest and the Intergalactic Medium [2][4]. The neutral hydrogen component of gas in the Inter Galactic Medium (IGM) and Circum Galactic Medium (CGM) covers column densities from 10^{14} to 10^{19} cm^{-2}, but most of the H I will be in the Lyman Limit Regime at column densities between 10^{17} and 10^{19} cm^{-2}. Although much is unknown about Lyman Limit Systems, they form the link between galaxies and their extended environment, the intergalactic medium, and they play an essential role in galaxy formation.

We can image the distribution of stars and gas in detail and measure the kinematics and rotation curves of galaxies, however on the topic of galaxy formation, there are many open questions related to the environment of galactic structures, which is an almost unexplored region. The halos are the regions where gas is accreting and where feedback processes can exchange material between the galaxy and the intergalactic medium (IGM). These circulation processes determine the life cycle of galaxies and are therefore vital to understand.

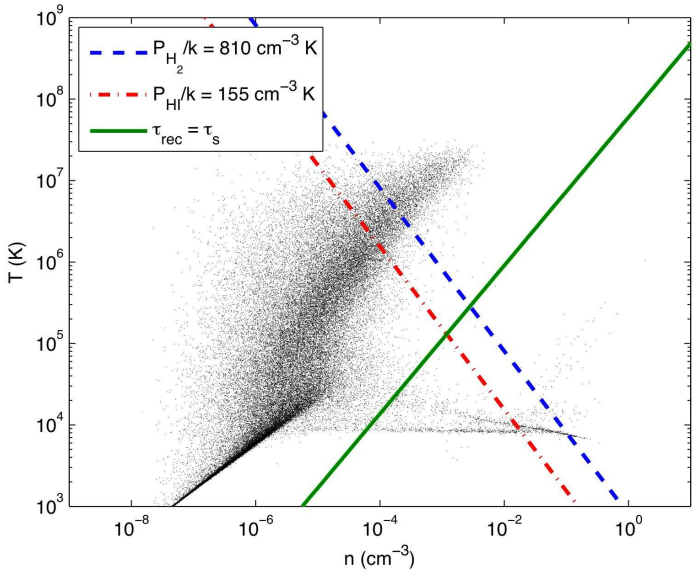

Figure 1: Phase diagram of particles in the numerical simulation. The dashed (blue) and dash-dotted (red) lines correspond to constant thermal pressures of $P/k = 155$ and 810 cm^{-3} K, that were found empirically to reproduce the observed mass densities of atomic and molecular gas at $z = 0$. Gas particles on the right side of the dashed blue line are considered molecular, while particles in between the two pressure lines and below the solid line are considered self-shielded and the neutral fraction is set to unity. The solid (green) line shows where the recombination time is equal to the sound-crossing time at a physical scale of one kpc. Particles above/left of the green line are unlikely to be neutral or molecular.

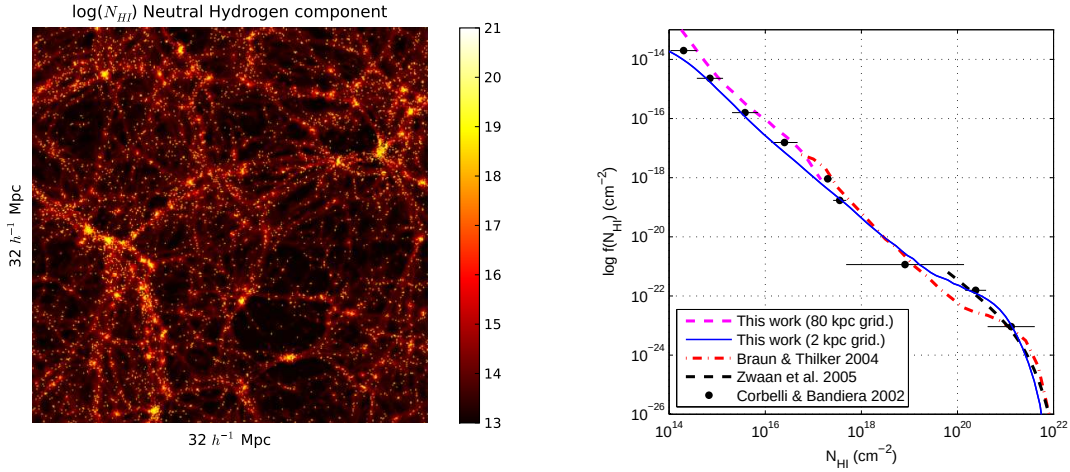

Figure 2: Left panel: Column density map of the H I component of the numerical simulation over a depth of 32 h^{-1} Mpc on a logarithmic scale, gridded to a resolution of 80 kpc. Right panel: H I distribution function of the simulation, gridded to a resolution of 2 kpc (solid blue line) and 80 kpc (dashed purple line)[7]. Overlaid are distribution functions from observational data of M31 [1], WHISP [9] and QSO absorption lines[3].

2. Numerical simulations

Numerical simulations are not limited by sensitivity and can help to predict and understand observations. We have employed a hydrodynamic simulation as described in [5] and [6] with a box size of 32 h^{-1} Mpc on each side to reconstruct the neutral hydrogen component of the Cosmic Web. At low densities the neutral fraction of the gas is determined by the balance between ionisation and recombination. We use a threshold in thermal pressure to correct for molecular (H_2) gas and self shielded gas as shown in Fig. 1 and explained in [7]

The integrated map of the reconstructed neutral hydrogen is shown in the left panel of Fig. 2, gridded to a voxel size of 80 kpc. Bright nodes can be recognised that represent the clusters and galaxies, connected by extended filaments with H I column densities of $10^{16} - 10^{17}$ cm^{-2}. High density regions were gridded to a 2 kpc, resolution to be able to resolve substructures and higher column density regions.

The statistical properties of the reconstructed neutral hydrogen are compared with observations to assess the reliability of the simulation. We find good correspondence when looking at the H I mass function, the two-point correlation function and the H I distribution function which is shown in the right panel of Fig. 2. The simulated H I distribution robustly describes the full column density range between $N_{HI} \sim 10^{14}$ and $N_{HI} \sim 10^{22}$ cm^{-2}.

3. Observations

To observe the environment of galaxies in neutral hydrogen, a very good brightness sensitivity is required that probes the regime of Lyman Limit Systems between $N_{HI} \sim 10^{17}$ and $N_{HI} \sim 10^{19}$ cm^{-2}. We have conducted three independent wide-field blind H I surveys using WSRT data in both

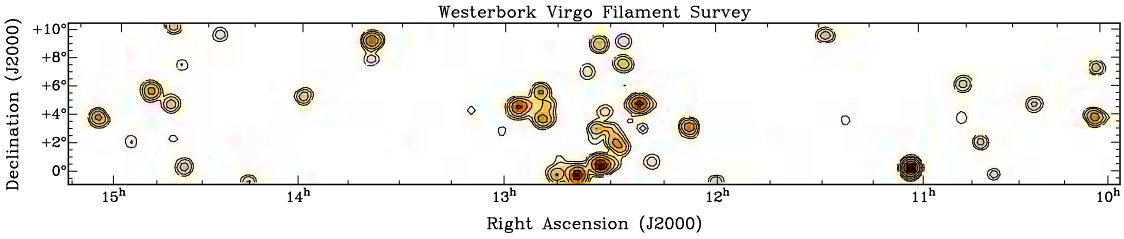

Figure 3: Illustration of the central 110 degrees of the WVFS region and detections in the velocity interval $400 < V_{Hel} < 1600$ km s^{-1}. The plot shows the integrated brightness levels, with contour levels drawn at 5 10, 20, 40, 80 and 160 Jy Beam^{-1} km s^{-1}.

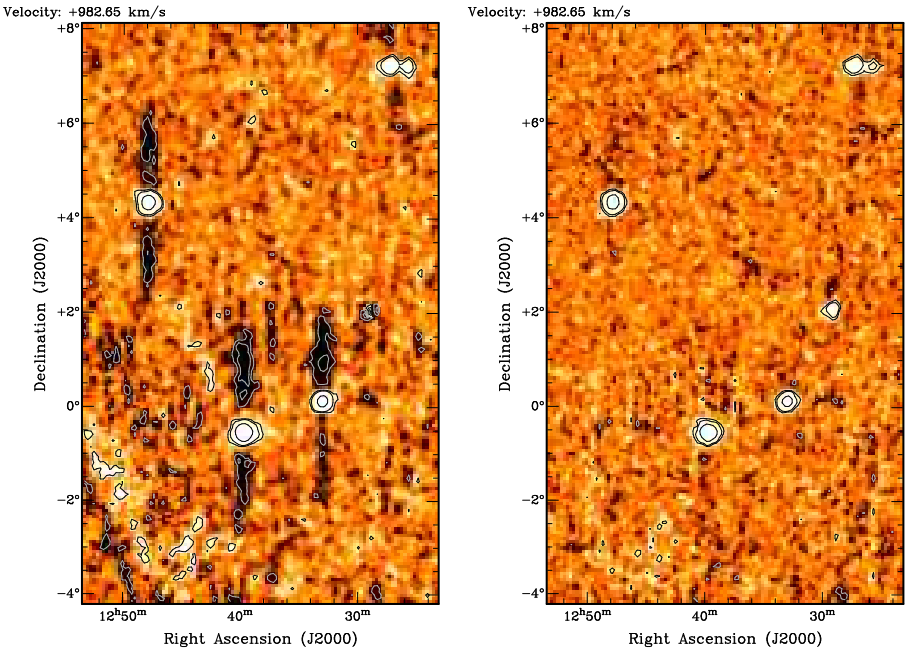

Figure 4: Example of the bandpass side-lobes in the original HIPASS pipeline (*left panel*) and the reprocessed data (*right panel*). Both panels show the same region on the sky and the same velocity, the intensity ranges from -40 to 40 mJy beam^{-1}. Contours are plotted at -60, -30, 30, 60 and 300 mJy beam^{-1}, negative contours are coloured white.

total-power and cross-correlation mode and by using re-processed HIPASS data. All three surveys map the galaxy filament joining the Virgo Cluster to the Local Group, extending from 8 to 17 hours in RA and from -1 to +10 degrees in Dec. out to a distance of $\sim$25 Mpc, an overview of the central region is shown in Fig. 3

I.) With the WSRT we have conducted the Westerbork Virgo Filament Survey (WVFS). When using the interferometer as an array of 14 single dish telescopes we achieve a 1σ surface brightness sensitivity of $N_{HI} \sim 3.5 \times 10^{16}$ cm^{-2} in a 49' beam [8].

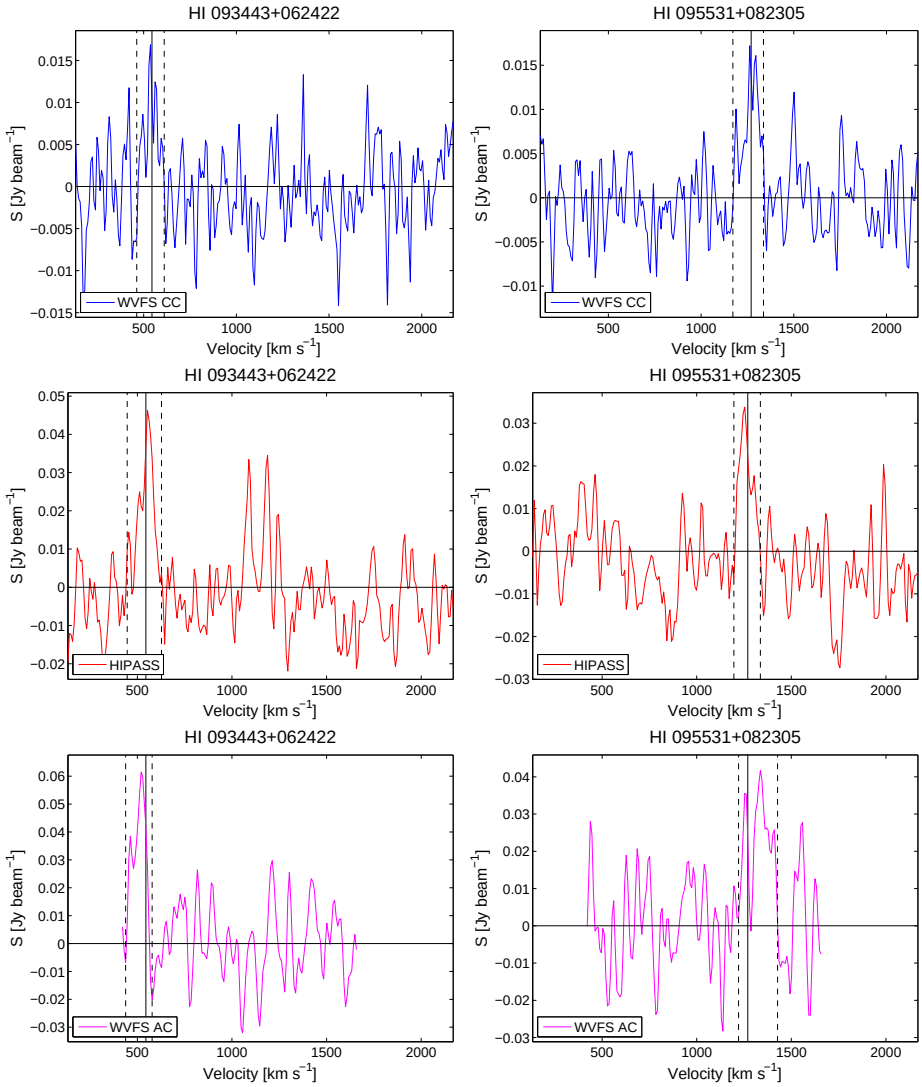

Figure 5: For two of the new H I detections three spectra are shown derived from the different surveys. The top panels show the WVFS cross-correlation spectrum, the middle panel the reprocessed HIPASS spectrum and the bottom panel the WVFS total-power spectrum.

II.) We have re-processed the original HIPASS data overlapping the WVFS data using an improved pipeline. Most negative artifacts around bright objects that were apparent in the original HIPASS product can be removed (Fig. 4). We achieve a 1σ surface brightness sensitivity of $N_{HI} \sim 3 \times 10^{17}$ cm^{-2} in a 15' beam [8].

III.) By observing with the WSRT at very extreme hour angles, a filled aperture can be simulated in projection, reaching the sensitivity of a single dish-telescope and the well defined bandpass characteristics of an interferometer. The observations and data reduction are described in detail in [8], a brightness sensitivity is reached of $N_{HI} \sim 10^{18}$ cm^{-2} in a 6' beam.

By comparing the three data sets with different angular resolutions, we can directly confirm

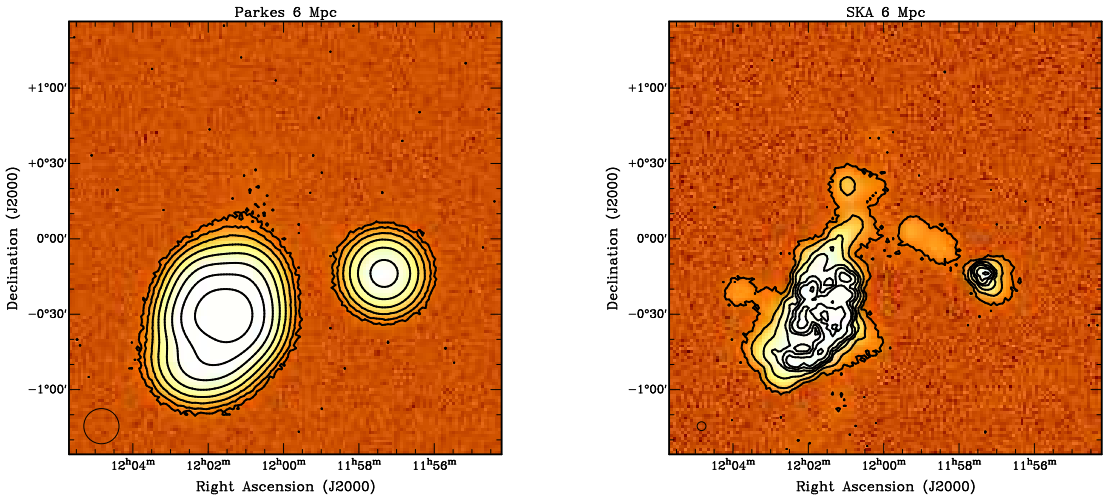

Figure 6: Mock observations created from the simulation after adding noise. The same object is shown using Parkes (left) and the SKA (right). Contour levels start at 3σ after 500 hours of observation time of a 30 square degree field. In the SKA image extended features and filaments can be identified, which are invisible in the Parkes observations

tentative objects when observed in more than one survey. We find 32 new detections of H I, of which 16 do not have a clear optical counterpart. As an example the three different spectra for two detections are shown in Fig. 5. The different spatial scales can give an estimate of the extent of a feature. An object with more flux in the low resolution data is probably diffuse and extended. A source with more flux in the high resolution data on the other hand is more likely a compact and denser object, that becomes diluted at lower angular resolution. The angular resolution of our observations is not sufficient to resolve the transition from high to low column densities. It appears that the detected Cosmic Web features have a relative dense core, outside this dense core there is extended neutral hydrogen up to a radius of $\sim$100 kpc.

4. Discussion

Both simulations and observations confirm that there is a significant amount of baryonic matter in the IGM and extended neutral hydrogen can be found when exploring Lyman Limit column densities between 10^{16} and 10^{19} cm^{-2}.

Observing large fractions of the sky down to a lower column density limit than presented in this work is not very realistic with existing telescopes. By using new techniques, the next generation of radio telescopes can observe the sky significantly faster and deeper. SKA pathfinders such as ASKAP and APERTIF will be able to map the full sky to a brightness sensitivity of only a few times 10^{18} cm^{-2} over a 3' beam. These sensitivity limits are comparable to the WVFS-CC limits, however at much higher resolution and better quality. Such an all sky survey will result in many new detections of Lyman Limit systems. Selected features can be followed up with more targeted telescopes, using e.g. MeerKAT. Only the SKA will be able to really map filaments connecting galaxies in detail. In Fig. 6 a prediction is shown from [7] of what a galaxy could look like when observed with the SKA.

References

[1] Braun, R., & Thilker, D. A. 2004, A&A, 417, 421

[2] Cen, R. & Ostriker, J. P. 1999, ApJ, 514, 1

[3] Corbelli, E. & Bandiera, R. 2002, ApJ, 567, 712

[4] Davé, R., Cen, R., Ostriker, J.P. et al. 2001, ApJ, 552, 473

[5] Oppenheimer, B. D. & Davé, R. 2006, MNRAS, 373, 1265

[6] Oppenheimer, B. D. & Davé, R. 2008, MNRAS, 387, 577

[7] Popping, A., Davé, R., Braun, R. & Oppenheimer, B. D. 2009, A&A, 504, 15

[8] Popping, A. 2010, PhD thesis, University of Groningen

[9] Zwaan, M. A., van der Hulst, J.M., Briggs, F.H., Verheijen, M. A. W., & Ryan-Weber, E. V. 2005, MNRAS, 364, 1467